Journal of Applied Mechanics and Technical Physics, Vol. 40, No. 3, 1999

AXIAL JET IN A POTENTIALLY ROTATING FLUID IN A PIPE OF VARIABLE RADIUS

V. N. Nikulin

UDC 532.5

Steady fluid flow in a jet located along the symmetry axis of a potentially rotating flow in a pipe of variable radius is considered. A theoretical model for this flow is constructed. The dependence of the jet parameters on the axial coordinate is investigated in a rigorous formulation under specified entry conditions. In particular, the extensibility or nonextensibility of the solution onto a semi-infinite interval is established. From an analysis of the behavior of the jet, an attempt is undertaken to estimate the behavior of the core of a tornado-like vortex in a pipe of variable radius, namely the possibility of breakdown or jump of the vortex.

The theoretical model is constructed using the approach developed in previous papers [1, 2], where fluid flow in the cores of vertical tornado-like vortices was considered. In contrast to [1, 2], where the flow dynamics is due to gravity, the dynamics in the present case is governed by the interaction of the flow in the axial jet with the surrounding rotating flow. As a result, we have a greater variety of possible motions than in [1, 2]. The approach developed here is based on conventional assumptions, such as an ideal fluid and a long-wave approximation. Within the framework of the indicated assumptions, all results are rigorous.

In the present paper, we study a nonrotating axial jet in a potentially rotating flow of the ambient fluid. It is assumed, however, that the fluid flow in the jet can qualitative reflect some important regularities of the axial fluid flow in the core of a tornado-like vortex, although the rotation of the fluid in the vortex core is close to rigid-body rotation. This is due to the fact that the pipe flow outside the vortex core is almost potentially rotational, and inside the core it has a jet character [3–5]. At the same time, within the framework of the problem considered, the following two factors are taken into account: rotation of the outer flow and its interaction with the jet flow. Both these factors can have a significant influence on the fluid flow in the core of a tornado-like vortex. Thus, theoretical results for the jet would be expected to agree, at least qualitatively, with experimental data for tornado-like vortices in pipes of variable radius. Such a comparison will be performed at the end of the paper. As a result, the influence of the mechanism considered on the flow in the vortex core is estimated.

1. Formulation of the Problem. An incompressible, inviscid, homogeneous fluid is considered. The flow is considered steady and rotationally symmetric. We introduce cylindrical coordinates (r, φ, z), where r is the radius, φ is the azimuth angle, and the z axis is directed along the symmetry axis. The fluid occupies a region $z \geqslant 0$, $r \leqslant r_0(z)$, where $r_0(z)$ is the radius of the pipe, a specified function of z. The flow is divided into two regions: region I $[r \leqslant r_1(z)]$ and region II $[r_1(z) \leqslant r \leqslant r_0(z)]$. Region I is the jet and region II is the outer flow. At the boundary r_1, discontinuity of the velocity component tangent to the boundary can occur. The flow parameters at $z = 0$ are considered known. The flow evolution as a function of the z coordinate is investigated.

To transform to dimensionless quantities, we introduce length, velocity, and density scales. The unit of length is the characteristic scale of variation along the z axis; the unit of velocity is the rotational velocity

Lavrent'ev Institute of Hydrodynamics, Siberian Division, Russian Academy of Sciences, Novosibirsk 630090. Translated from Prikladnaya Mekhanika i Tekhnicheskaya Fizika, Vol. 40, No. 3, pp. 81–89, May–June, 1999. Original article submitted January 5, 1998; revision submitted July 14, 1998.

0021-8944/99/4003-0431 $22.00

component in region II at $z = 0$ and $r = r_0$; the fluid density is equal to unity. Below, all quantities are used in dimensionless form unless otherwise specified.

The following notation is used: (u, v, w) are velocity components that correspond to (r, φ, z), p is the pressure, and δ is the dimensionless value of r_0 at $z = 0$. It is assumed that $\delta \ll 1$, i.e., the radius of the pipe varies slowly with variation of the z coordinate.

Passing over to a long-wave approximation, we extend the coordinates and functions [1]:

$$r^2 \to \delta^2\eta, \qquad z \to z, \qquad 2ur \to \delta^2 q, \qquad vr \to \delta A, \qquad w \to w, \qquad p \to p.$$

Thus, the boundaries $r_0(z)$ and $r_1(z)$ transform into $\eta_0(z)$ and $\eta_1(z)$, and $\eta_0(0) = 1$, according to the definition of δ.

As a result, the equations of motion and continuity take the form

$$\begin{gathered} qw_\eta + ww_z = -p_z, \qquad \frac{\delta^2}{2}\Big(qq_\eta - \frac{q^2}{2\eta} + wq_z\Big) - \frac{A^2}{\eta} = -2\eta p_\eta, \\ qA_\eta + wA_z = 0, \qquad q_\eta + w_z = 0. \end{gathered} \tag{1.1}$$

The subscripts from independent variables denote the corresponding partial derivatives.

The boundary conditions are

$$q = A = 0 \quad \text{for} \quad \eta = 0. \tag{1.2}$$

At the boundary of the regions $\eta = \eta_1$, the pressure is considered continuous and the following kinematic condition

$$q = w\eta_{1z} \tag{1.3}$$

is satisfied. For $\eta = \eta_0$, the nonpenetration condition is satisfied:

$$q = w\eta_{0z}. \tag{1.4}$$

Furthermore, the terms in (1.1) that are multiplied by δ^2 are considered small and are omitted, and the system is transformed to mixed Euler–Lagrange variables in the same manner as is done in [1, 2]. The transformation of the equations is performed separately for regions I and II.

The new independent variables z' and ν $(0 \leqslant \nu \leqslant 1)$ are introduced by the relations $z = z'$ and $\eta = R(z', \nu)$, where R satisfies the equation

$$wR_{z'} = q \tag{1.5}$$

and the boundary conditions

$$\begin{gathered} R(z', 0) = 0, \qquad R(z', 1) = \eta_1, \qquad R(0, \nu) = \nu\eta_{10} \quad \text{in region I;} \\ R(z', 0) = \eta_0, \qquad R(z', 1) = \eta_1, \qquad R(0, \nu) = (1 - \nu) + \nu\eta_{10} \quad \text{in region II.} \end{gathered}$$

Here $\eta_{10} = \eta_1(0)$ and it is taken into account that $\eta_0(0) = 1$. With this definition of R, boundary conditions (1.2) (for q) and (1.3), and (1.4) are satisfied automatically. The unknown boundary η_1 becomes the known boundary $\nu = 1$. If we ignore the terms with δ^2, system (1.1) in the variables z' and ν (below, the prime on z' is omitted) takes the form

$$wA_z = 0, \quad \frac{A^2}{2R^2}R_\nu = p_\nu, \quad R_\nu ww_z = -R_\nu p_z + R_z p_\nu, \quad q_\nu + R_\nu w_z - R_z w_\nu = 0.$$

From the first equation it follows that $A = A(\nu)$. Then, integration of the second equation with respect to ν from ν to 1 yields an expression for p, and the result is substituted into the third equation. By means of (1.5), q is eliminated from the fourth equation. As a result, we obtain the following system of two equations:

$$ww_z = -p_{1z} - (A_1^2/(2R_1))_z + \Big(\int_\nu^1 (2R)^{-1}(A^2)_\nu d\nu\Big)_z, \qquad (wR_\nu)_z = 0. \tag{1.6}$$

Here A_1, p_1, and R_1 are values that correspond to $\nu = 1$ (at the boundary between regions I and II). We note that the equations have the same form (1.6) in regions I and II. The values of A_1 can be different since in passage through the boundary, a jump in the velocity component tangent to the boundary is admissible. The values of p_1 and R_1 are the same in regions I and II because of the pressure continuity and the definition of R.

We first construct a solution in a special form in region II:

$$w = w_2(z), \qquad A = 1, \qquad R = (1-\nu)\eta_0(z) + \nu\eta_1(z). \tag{1.7}$$

We note that solutions (1.7) are a good approximation of real flows outside the vortex core [5]. Substituting (1.7) into (1.6), we obtain p_{1z}:

$$-2p_{1z} = (1/\eta_1)_z + (w_{20}^2(1-\eta_{10})^2/(\eta_0-\eta_1)^2)_z.$$

Here $w_{20} = w_2(0)$, $\eta_{10} = \eta_1(0)$, and $\eta_0(0) = 1$. The resulting value of p_{1z} is substituted into system (1.6) for region I. As a result, for region I we obtain the equations

$$\left\{w^2 + \frac{A_1^2 - 1}{\eta_1} - w_{20}^2\frac{(1-\eta_{10})^2}{(\eta_0-\eta_1)^2} - \int_\nu^1 R^{-1}(A^2)_\nu\, d\nu\right\}_z = 0, \qquad (wR_\nu)_z = 0, \tag{1.8}$$

where A_1 is the value of A for $\nu = 1$ in region I (generally, it is not equal to 1); the quantity R_1 is replaced by η_1. Thus, the study of the flow in the jet was reduced to the study of the behavior of the solutions of system (1.8). Equations (1.8) are solved with initial data for $z = 0$.

A system of equations qualitatively similar to (1.8) is obtained and studied in [1, 2]. It is shown that the equations are considerably simplified and rigorous analytical estimates are obtained if the integral term in the first equation is equal to zero. In this case, as shown in [2], the main regularities of the behavior of the vortex core are the same in the presence or absence of this term. Thus, to understand the main regularities, we originally restrict ourselves to the case $A_\nu = 0$. It is easy to see that the condition $A_\nu = 0$ leads to the condition $A = 0$, i.e., in this case, the fluid in the jet does not have a vorticity component along the axis.

We set $A = 0$ (hence, $A_1 = 0$). We integrate (1.8) from 0 to z. Next, the first equation is solved for η_0. Integration of the second equation with respect to ν with allowance for the fact that $\eta_1 = R(z,1)$ yields an expression for η_1. As a result, we have

$$\begin{gathered}\eta_0 = f(\psi), \qquad f(\psi) = w_{20}(1-\eta_{10})(w_{20}^2 + \psi - 1/\eta_1 + 1/\eta_{10})^{-1/2} + \eta_1, \\ \eta_1 = \int_0^1 w_0(\nu)\eta_{10}(w_0^2 + \psi)^{-1/2}\, d\nu.\end{gathered} \tag{1.9}$$

Here the following notation is used: $\psi = w^2 - w_0^2$, where w_0 is the value of w for $z = 0$.

Thus, the problem amounts to the study of the dependence $\psi(\eta_0)$, which is given in an implicit manner by Eqs. (1.9).

2. Structure of the Solutions. We first examine the dependence of ψ (and, hence, w and η_1) on η_0 for small variations of η_0 in the vicinity of $\eta_0 = 1$ ($\eta_0 = 1$ at $z = 0$); $\psi(1) = 0$, according to the definition of ψ. In the neighborhood of zero, the behavior of $f(\psi)$ is determined by the value of the first derivative at zero. Then, $\psi \approx (\eta_0 - 1)/\lambda$ for $\psi \ll 1$, where

$$\lambda = f'(0) = \frac{1-\eta_{10}}{2w_{20}^2}\left(\frac{1}{\eta_{10}}\int_0^1 \frac{d\nu}{2w_0^2} - 1\right) - \int_0^1 \frac{\eta_{10}\, d\nu}{2w_0^2}.$$

Hence it follows that the behavior of ψ with variation in η_0 is qualitatively different, depending on the sign of λ. For example, for $\lambda > 0$, as η_0 (i.e., the radius of the nozzle) increases, ψ and w increase, and η_1 decreases; for $\lambda < 0$, ψ and w decrease, and η_1 increases.

We study the nonlinear stage of the dependence $\psi(\eta_0)$. For this, we examine the properties of the function $f(\psi)$. We assume that $w_0(\nu)$ satisfies the inequalities $0 < \gamma \leqslant w_0(\nu) < \infty$. Let $f'(0) \neq 0$. Then,

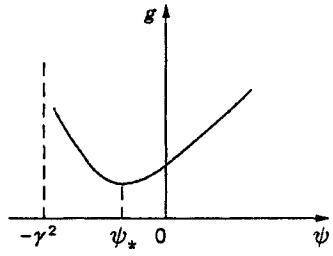

Fig. 1

by virtue of the implicit function theorem and the definitions of η_1 and $f(\psi)$ and with allowance for the restrictions on $w_0(\nu)$, Eqs. (1.9) have solutions as long as $f'(\psi) \neq 0$, $\psi \geqslant -\gamma^2$, and $f(\psi)$ is bounded. We introduce the notation $g(\psi) = w_{20}^2 + \psi - 1/\eta_1 + 1/\eta_{10}$. Then,

$$f(\psi) = w_{20}(1 - \eta_{10})g^{-1/2} + \eta_1. \tag{2.1}$$

Differentiating $g(\psi)$, we obtain

$$g'(\psi) = 1 - \eta_1^{-2} \int_0^1 (w_0\eta_{10}/2)(w_0^2 + \psi)^{-3/2}\, d\nu,$$

$$g''(\psi) = \frac{3}{4\eta_1^2} \int_0^1 \frac{w_0\eta_{10}\, d\nu}{(w_0^2 + \psi)^{5/2}} - \frac{1}{2\eta_1^3}\left(\int_0^1 \frac{w_0\eta_{10}\, d\nu}{(w_0^2 + \psi)^{3/2}}\right)^2.$$

Using the Cauchy–Bunyakovskii inequality, it is easy to show [1] that $g''(\psi) > 0$. Thus, $g(\psi)$ is a downward convex function. In addition, we assume that $g'(-\gamma^2) < 0$ [for physically real flows, this inequality is always satisfied since $g'(\psi) \to -\infty$ as $\psi \to -\gamma^2$ by virtue of the divergence of the integral]. Obviously, $g'(\psi) \to 1$ as $\psi \to \infty$. Then, from the convexity of $g(\psi)$ it follows that there is a unique value $\psi = \psi_*$ such that $g'(\psi_*) = 0$. There are four qualitatively different forms of the function $g(\psi)$:

q1) $g'(0) > 0$, $\psi_* < 0$, $g(\psi_*) > 0$;
2) $g'(0) > 0$, $\psi_* < 0$, $g(\psi_*) < 0$;
3) $g'(0) < 0$, $\psi_* > 0$, $g(\psi_*) > 0$;
4) $g'(0) < 0$, $\psi_* > 0$, $g(\psi_*) < 0$.

The first form is shown in Fig. 1. The remaining forms differ from it by a shift of the plot downward (so that the minimum falls below the abscissa), to the right ($\psi_* > 0$), and to the lower right.

The behavior of $g(\psi)$ depends on the form of $f(\psi)$. From (2.1) it follows that

$$f'(\psi) = -(w_{20}(1 - \eta_{10})g^{-3/2}/2)g'(\psi) + \eta_1'(\psi). \tag{2.2}$$

Case I. Let $g'(0) > 0$. Then, $g'(\psi) > 0$ for $\psi > 0$. Since $\eta_1'(\psi) < 0$, we have $f'(\psi) < 0$ for $\psi > 0$. Thus, $f(\psi)$ is a monotonically decreasing function for $\psi > 0$ and $f(\psi) \to 0$ as $\psi \to \infty$. Hence it follows that Eqs. (1.9) have a unique solution $\psi(\eta_0)$ if η_0 decreases. Thus, with decrease in η_0, ψ and w increase and η_1 decreases.

We study the behavior of $f(\psi)$ for $\psi < 0$, assuming as before that $g'(0) > 0$.

1. Let $g(\psi_*) > 0$. Then, the following two cases are possible:

(a) $f'(\psi) < 0$ for all $\psi < 0$ down to $\psi = -\gamma^2$. Then, $f(\psi)$ is a monotonically decreasing function over the entire interval $\psi > -\gamma^2$. Hence it follows that (1.9) has a unique solution for all $\eta_0 < \eta_{0*}$, where η_{0*} is defined by the equation $\eta_{0*} = f(-\gamma^2)$; ψ and w are monotonically decreasing functions of η_0, and η_1 is an increasing function. For $\eta_0 > \eta_{0*}$, solutions do not exist. Solutions cease to exist because $w(\nu)$ vanishes at points ν at which $w_0(\nu) = \gamma$. Qualitatively, the plot of $f(\psi)$ is shown in Fig. 2a (curve 1).

(b) $f'(\psi) < 0$ for all $\psi > \psi_1$, where $f'(\psi_1) = 0$ and $-\gamma^2 < \psi_1 < 0$. Then, by virtue of the implicit function theorem, a solution of (1.9) exists only for $\eta_0 \leqslant \eta_{01}$, where $\eta_{01} = f(\psi_1)$. Here the dependence of ψ

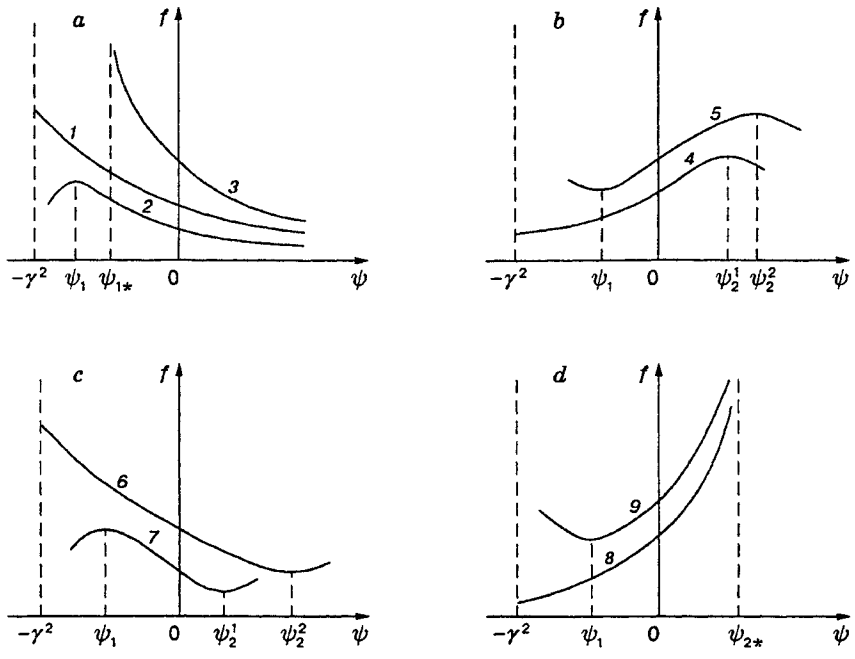

Fig. 2

on η_0 also decreases monotonically over the entire interval $\eta_0 > \eta_{01}$. The solution ceases to exist for $\eta_0 \to \eta_{01}$ because the derivatives of ψ with respect to η_0 tend to infinity (curve 2 in Fig. 2a).

2. Let now $g(\psi_*) < 0$. Then there is ψ_{1*} ($\psi_* < \psi_{1*} < 0$) such that $g(\psi_{1*}) = 0$, $f(\psi) \to \infty$ as $\psi \to \psi_{1*}$, and $f'(\psi) < 0$ for $\psi \geqslant \psi_{1*}$. Hence it follows that a solution exists for all η_0. In this case too, ψ is a monotonically decreasing function η_0, and $\psi \to \psi_{1*}$ as $\eta_0 \to \infty$ (curve 3 in Fig. 2a).

Thus, if $g'(0) > 0$, three cases of the behavior of $\psi(\eta_0)$ are possible: I.1a, I.1b, and I.2. We examine the properties of $f(\psi)$ for $g'(0) < 0$.

Case II. Let $g'(0) < 0$. In this case, by virtue of (2.2) and the inequalities $\eta_1'(\psi) < 0$, the following two cases are possible: $f'(0) > 0$ and $f'(0) < 0$.

1. Let $f'(0) > 0$ and $g(\psi_*) > 0$. Because $g'(\psi)$ increases up to zero with increase in ψ, and $\eta_1' < 0$, there is $\psi_2 > 0$ (ψ_2^1 and ψ_2^2 in Fig. 2b) such that $f'(\psi_2) = 0$. Then, by virtue of the implicit function theorem, a solution exists for $\psi > 0$ only when $\psi < \psi_2$. For $\psi < 0$, the following two cases are possible:

(a) $f'(\psi) > 0$ for all $-\gamma^2 \leqslant \psi \leqslant 0$, then a solution exists up to $\psi = -\gamma^2$ (curve 4 in Fig. 2b);

(b) $f'(\psi)$ vanishes for $-\gamma^2 < \psi_1 < 0$, and then a solution exists up to $\psi = \psi_1$ (curve 5 in Fig. 2b)

In both cases, ψ increases with increase in η_0 and a solution exists on a bounded segment $\eta_{01} < \eta_0 < \eta_{02}$, where $\eta_{02} = f(\psi_2)$ ($\psi_2 = \psi_2^1$ and $\psi_2 = \psi_2^2$ for curves 4 and 5, respectively) and η_{01} is equal to $f(-\gamma^2)$ or $f(\psi_1)$. The solution ceases to exist for $\eta_0 \to \eta_{02}$ because the derivatives tend to infinity and for $\eta_0 \to \eta_{01}$ because the axial velocity inside the core vanishes (case II.1a) or the derivatives tend to infinity (case II.1b) (Fig. 2b).

2. Let $f'(0) < 0$ and $g(\psi_*) > 0$. Then, two new cases for $f(\psi)$ are possible:

(a) $f'(\psi) < 0$ for $-\gamma^2 < \psi < \psi_2^2$, where $0 < \psi_2^2 < \infty$ and $f'(\psi_2^2) = 0$ (curve 6 in Fig. 2c);

(b) $f'(\psi) < 0$ for $\psi_1 < \psi < \psi_2^1$, where $-\gamma^2 < \psi_1 < 0$, $0 < \psi_2^1 < \infty$, and $f'(\psi_1) = f'(\psi_2^1) = 0$ (curve 7 in Fig. 2c).

3. Let $g'(0) < 0$ and $g(\psi_*) < 0$. Since $\psi_* > 0$ for $g'(0) < 0$, the types of behavior of $f(\psi)$ for $\psi < 0$ are the same as in cases II.1 and II.2. For $\psi > 0$, differences appear. Since $g(0) > 0$, $g(\psi_*) < 0$, and $\psi_* > 0$, there is ψ_{2*} such that $g(\psi_{2*}) = 0$, where $0 < \psi_{2*} < \psi_*$. Since $g(\psi_{2*}) = 0$, from (2.1) it follows that $f(\psi) \to \infty$ as $\psi \to \psi_{2*}$.

Let $f'(0) > 0$. Then, if $f'(\psi) > 0$ for $0 < \psi < \psi_{2*}$, two new cases are possible:

(a) a solution exists for all $\eta_0 > f(-\gamma^2)$ (curve 8 in Fig. 2d);

(b) a solution exists for all $\eta_0 > f(\psi_1)$, where ψ_1 is such that $f'(\psi_1) = 0$ (curve 9 in Fig. 2d).

In both cases, ψ increases with increase in η_0 and $\psi \to \psi_{2*}$ as $\eta_0 \to \infty$.

Let $f'(0) < 0$. Hence it follows that near zero, $f(\psi)$ decreases as ψ increase. Since $f(\psi) \to \infty$ as $\psi \to \psi_{2*}$, there exists ψ_2 such that $f'(\psi_2) = 0$, where $0 < \psi_2 < \psi_{2*}$. Thus, cases II.2a and II.2b are realized, and new cases will not arise.

Thus, the following statements are proved:

— For $g'(0) > 0$ and $g(\psi_*) > 0$, a solution $\psi(\eta_0)$ exists for η_0 from the interval $0 < \eta_0 < \eta_{01}$, where η_{01} is equal to $f(-\gamma^2)$ or $f(\psi_1)$. In this case, $\psi'(\eta_0) < 0$;

— For $g'(0) > 0$ and $g(\psi_*) < 0$, a solution exists for all η_0 and $\psi'(\eta_0) < 0$;

— For $g'(0) < 0$, $f'(0) > 0$, and $g(\psi_*) > 0$, a solution exists for η_0 from the interval $\eta_{01} < \eta_0 < \eta_{02}$, where η_{01} is equal to $f(-\gamma^2)$ or $f(\psi_1)$, and $\eta_{02} = f(\psi_2^1)$ in case II.1a and $\eta_{02} = f(\psi_2^2)$ in case II.1b, $\psi'(\eta_0) > 0$;

— For $g'(0) < 0$, $f'(0) > 0$, and $g(\psi_*) < 0$ a solution exists for η_0 from the interval $\eta_{01} < \eta_0 < \infty$ and $\psi'(\eta_0) > 0$;

— For $g'(0) < 0$ and $f'(0) < 0$, a solution exists for η_0 from the interval $\eta_{02} < \eta_0 < \eta_{01}$ and $\psi'(\eta_0) < 0$.

In divergent nozzles, a solution for all $\eta_0 \to \infty$ exists only in three cases: I.2, II.3a, and II.3b. In case I.2, ψ and w decrease, and the jet radius η_1 increases to finite values as $\eta_0 \to \infty$. In cases II.3, ψ and w increase, and the jet radius decreases to finite values as $\eta_0 \to \infty$. In convergent nozzles, a solution exists for all $\eta_0 \to 0$ in three cases: I.1a, I.1b, and I.2. For all η_0 from 0 to ∞, a solution exists only if case I.2 is realized.

The case of a thin jet is a certain simplification of the problem. We assume that the jet radius is much smaller than the radius of the pipe ($\eta_1 \ll \eta_0$). Then, ignoring η_1 compared to η_0, we omit η_1 on the right side of the second equation of (1.9) and η_{10} in the expression $1 - \eta_{10}$. As a result, we find that the signs of $f'(\psi)$ and $g'(\psi)$ are opposite. It is easy to see that, thus, of the indicated nine cases, only the following four remain: I.1b, I.2, II.1a, and II.3a. We note that in cases I.1b and I.2, the dependence of the jet radius on the nozzle radius increases monotonically, and in cases II.1a and II.3a, it decreases monotonically. Thus, in convergent nozzles, a solution exists up to $\eta_0 \to 0$ in cases I.1b and I.2, and in divergent nozzles, it exist up to $\eta_0 \to \infty$ in cases I.2 and II.3a.

3. Comparison of the Theory with Experiments. Within the framework of the proposed model, the flow evolution in the jet along the axis is calculated as a function of the nozzle radius. For this, according to (1.9), it is necessary to know the following parameters at the nozzle entry: the jet radius, the velocity circulation around the axis in the outer flow, and the axial velocities in the outer flow and the jet.

We compare the results obtained with experimental data on tornado-like vortices in pipes of variable radius in order to establish the influence of the mechanism considered on the vortex flow. Following [6], we assume that for a tornado-like vortex having the same entry parameters for the outer flow and axial velocity in the core as the jet, vortex breakdown or jump arises in the place of nonextensibility of the solution for the jet. In other words, the behavior of the vortex core is estimated from analysis of the jet behavior. We compare the estimates with the experiments of [4], where both the locations of vortex breakdown and velocity profiles were measured.

According to [4], the profiles of dimensional azimuthal and axial velocities in the vortex before breakdown have the form

$$V = (K/r)(1 - \exp(-\alpha r^2)), \qquad W = W_1 + W_2 \exp(-\alpha r^2), \tag{3.1}$$

where α, K, W_1, and W_2 are constants.

As the radius of the core, we use the value for which the rotational velocity component reaches a maximum. According to (3.1), this occurs for $\alpha r_1^2 \approx 1.25$. For analytic estimates, the axial velocities of the outer flow and the flow in the core are approximated by their values averaged over the cross section. From (3.1) it follows that the average axial velocity in the core is $W_0 = W_1 + W_2(1 - \exp(-\alpha r_1^2))/(\alpha r_1^2) \approx W_1 + 0.57W_2 = 0.43W_1 + 0.57W_{\max}$, where $W_{\max} = W_1 + W_2$ is the maximum axial velocity attained on the axis for $r = 0$. The velocities are normalized by $V_0 = K/r_{00}$ (r_{00} is the radius of the pipe at the entry). The values of W_1, $W_{\max}$, and K are taken from the plots given in [4, Fig. 2]. The quantity K is calculated from the data taken at a

TABLE 1

Flow parameters	Re							
	3220		4540			6000		
Ω	1.068	1.541	0.727	1.068	1.282	0.727	1.068	1.282
W_1	7.67	7.23	11	11	10.9	14.68	14.25	13.6
$W_{\max}$	12.27	15.9	16	20.25	22.5	21.9	27.84	32
W_0	10.29	12.17	13.85	16.27	17.51	18.8	22	24.09
V_0	3	4.23	3.12	4.29	5.25	4	5.92	7.12
r_{10}/r_{00}	0.31	0.31	0.29	0.29	0.29	0.28	0.28	0.28
$g'(0)$	0.56	0.37	0.7	0.59	0.47	0.71	0.54	0.45
$(r_*/r_{00})_t$	1.23	1.13	1.47	1.42	1.24	1.55	1.34	1.3
$(r_*/r_{00})_e$	1.25	1.04–1.09	—	1.19–1.24	1.10–1.14	—	1.15–1.18	1.04
$(z_*/r_{00})_t$	9.2	5.2	18.8	16.8	9.6	22	13.6	12
$(z_*/r_{00})_e$	9.6	1.7–3.2	—	7.6–9.2	3.9–5.7	—	5.8–7.0	1.7

distance of $0.8r_{00}$ since at the pipe walls, the rotational velocity component decreases abruptly and departure from law (3.1) takes place. Up to a distance of $0.8r_{00}$, the profiles of V are well approximated by relation (3.1). Then, $w_{20} = W_1/V_0$, and $w_0 = W_0/V_0$.

Integrating (1.9) and the expression for $g'(0)$ assuming that w_0 is constant, we obtain

$$g'(0) = 1 - 1/(2\eta_{10}w_0^2), \tag{3.2}$$

$$\eta_0 = w_{20}(1-\eta_{10})[w_{20}^2 + \psi - (w_0^2+\psi)^{1/2}/(w_0\eta_{10}) + 1/\eta_{10}]^{-1/2} + w_0\eta_{10}(w_0^2+\psi)^{-1/2},$$

where $\eta_{10} = (r_{10}/r_{00})^2$ (r_{10} is the radius of the core at the entry). Since in all plots [4, Fig. 2] $\eta_{10} < 0.1 \ll 1$, the calculations are performed in the approximation of a thin jet. This accuracy is sufficient to obtain estimates of the order of magnitude. In addition, as follows from (1.9) and [4, Fig. 2], for real axial velocity profiles, the integrand in the formula for η_1 is an integrable function as $\psi \to -w_0^2(\nu)$ for any ν. Hence it follows that η_1 has the same order of magnitude as η_{10} does. If the average value is taken as the w_0, then η_1 tends to ∞ as $\psi \to -w_0^2$, and this is inconsistent with the real situation. Ignoring the second term and η_{10} in the second equation of (3.2) compared to 1, after transformations we obtain

$$\eta_0 = f(\psi) \approx w_{20}\{[(w_0^2+\psi)^{1/2} - w_0(1-g'(0))]^2 + w_{20}^2 - (w_0g'(0))^2\}^{-1/2}. \tag{3.3}$$

From (3.3) it follows that the type of $f(\psi)$ is determined by the sign of $g'(0)$ and the sign of the difference $w_{20}^2 - (w_0g'(0))^2$. As shown below, they are both positive, i.e., $f(\psi)$ belongs to case I.1b. Thus, in a divergent pipe, the solution is extensible to a finite interval until $f(\psi)$ reaches a maximum. From (3.3) it follows that the maximum is reached when the expression in square brackets vanishes. Thus, we obtain the maximum pipe radius up to which a continuous solution exists. We assume that in the place of nonextensibility of the solution there is vortex breakdown or jump. Then, the pipe radius r_* and the distance along the z_* axis at which these phenomena take place are approximately equal to

$$r_*/r_{00} \approx w_{20}^{1/2}\{w_{20}^2 - (w_0g'(0))^2\}^{-1/4}, \qquad z_*/r_{00} \approx [(r_*/r_{00}) - 1]\cot\alpha, \tag{3.4}$$

where $\alpha = 1.43°$ (α is the half-angle of the pipe opening) and $\cot\alpha \approx 40$. Table 1 gives the values of W_1, $W_{\max}$, W_0, V_0 [cm/sec], r_{10}/r_{00}, Re, and Ω calculated on the basis of Fig. 2 in [4], the values of $g'(0)$, $(r_*/r_{00})_t$, and $(z_*/r_{00})_t$ calculated from formulas (3.2) and (3.4), and the experimental values of $(r_*/r_{00})_e$ and $(z_*/r_{00})_e$ obtained from the plots (see [4, Fig. 17]).

From Table 1 it follows that there qualitative agreement with the experiments. As indicated in [4],

for fixed Reynolds numbers, an increase in Ω shifts the vortex breakdown upstream, i.e., the breakdown arises at smaller radii of the pipe since the pipe diverges downstream. Although the model can be related to axisymmetric breakdown, calculations by formula (3.4) given in Table 1 show that an increase in Ω for a specified Re number leads to a decrease in $(r_*/r_{00})_t$ for the cases given [4, Fig. 2]. The calculated quantitative values were mostly larger than the experimental results, but they give estimates of the orders of magnitude. The more considerable differences for z_* compared to r_* are explained by the small opening angle of the pipe in the experiments and, as a consequence, by the high sensitivity of the axial position of the breakdown z_* to small variations in r_*.

Faler and Leibovich [4] pointed out that the dependence of the position of the vortex breakdown at a specified Ω on the Re number is not always monotonic. With increase in Re, it is more often shifted upstream, but, sometimes, downstream. According to the data of Table 1, the dependence of $(r_*/r_{00})_t$ on the Re number also does not exhibit strictly monotonic behavior.

We note that the calculation of $g'(0)$ and $g(\psi_*)$ from the experimental data for flows before vortex breakdown given in [5, Table 1] gives $g'(0) > 0$ and $g(\psi_*) > 0$. Hence it follows that flows before the breakdown refer to case I.1a or I.1b. In both cases, a continuous solution for divergent pipes exists, according to the model, only for bounded radii of the pipe, and this agrees qualitatively with the experiments.

Thus, one can conclude that the mechanism of interaction of the axial jet with the outer rotating flow considered in the model is manifested, at least, for given experimental data, in the fluid flow in the core of a tornado-like vortex in a pipe of variable radius. Account of this mechanism based on the study of the jet behavior allows one to predict the possibility of vortex breakdown and to evaluate its location.

The interaction of the axial jet with the outer rotating flow has a complicated character since even in the fairly exact formulation of the problem considered, a great number of possible types of flow dependent on the entry conditions are obtained.

REFERENCES

1. V. V. Nikulin, "Analog of shallow-water vortex equations for hollow and tornado-like vortices. The height of a steady tornado-like vortex," *Prikl. Mekh. Tekh. Fiz.*, No. 2, 47–52 (1992).
2. V. V. Nikulin, "Motion of a swirled fluid in the core of a vertical, tornado-like vortex," *Prikl. Mekh. Tekh. Fiz.*, **36**, No. 2, 81–87 (1995).
3. T. Sarpakaya, "Effect of the adverse pressure gradient on vortex breakdown," *AIAA J.*, **12**, No. 5, 602–607 (1974).
4. L. H. Faler and S. Leibovich, "Disrupted states of vortex flow and vortex breakdown," *Phys. Fluids*, **20**, No. 9, 1385–1400 (1977).
5. S. Leibovich, "The structure of vortex breakdown," *Annu. Rev. Fluid Mech.*, **10**, 221–246 (1978).
6. A. Mager, "Dissipation and breakdown of a win-tip vortex," *J. Fluid Mech.*, **55**, No. 4, 609–628 (1972).